

# Spectral analysis of EGRET pulsars

Fabio Gargano\* on behalf of LAT collaboration and the Pulsar Timing Consortium

\*Istituto Nazionale di Fisica Nucleare - Sez. Bari Via Orabona 4 - 70126 - Bari -Italy

**Abstract.** The Large Area Telescope (LAT) is the main instrument on board the *Fermi* Gamma-ray Space Telescope, launched on June 11<sup>th</sup> 2008. A significant improvement in sensitivity of the LAT over EGRET is due to its large field of view and effective area, combined with its excellent timing capabilities. One of the most promising topics of the mission is the study of pulsars. All EGRET pulsars have been detected in early weeks after launch and several new gamma-ray pulsars have been discovered so far. We focus the attention on the spectral emission of three of EGRET identified pulsars, namely B1055-52, B1706-44 and B1951+32 and compare the new results with the old ones.

**Keywords:** Gamma-ray astronomy, Gamma-ray astronomy detectors, Gamma-ray spectroscopy

## I. INTRODUCTION

The Large Area Telescope (LAT) was launched on June 11<sup>th</sup> 2008 on-board the *Fermi* Gamma-ray Space Telescope (formerly GLAST [1]). The LAT was built to address, along with other pressing questions in high energy astrophysics, the extent to which gamma-ray emission by pulsars is a rule, and thereby to better understand the mechanisms by which the kinetic energy of a rotating neutron star is transformed into intense beams of radiation.

The radio pulsar PSR B1055-52 [2] has a period of 197.11 ms and a period derivative of  $5.8 \times 10^{-15} \text{ s s}^{-1}$  and an average surface magnetic field of  $1.2 \times 10^{12} \text{ G}$ , a characteristic age of  $5.3 \times 10^5 \text{ yr}$  and a rotational energy loss rate of  $3.0 \times 10^{34} \text{ erg s}^{-1}$ . From the dispersion measure of  $30.1 \text{ pc cm}^{-3}$  and the mean free electron density, the distance is estimated to be 1.5 kpc. It was first detected as soft X-ray source by the *Einstein Observatory* [3], but the detection doesn't revealed modulation at the pulsar rotation frequency. The pulsation in the X-ray band was discovered by *ROSAT*. The first detection of gamma-ray pulsed emission was done by *EGRET* in 1993 [4].

The radio pulsar PSR B1706-44 was discovered in 1992 during a high frequency search of the southern sky [5]. In 1992 it was discovered by *EGRET* [6] as a gamma-ray pulsar. It has a period of 102.4 ms, a period derivative of  $93.0 \times 10^{-15} \text{ ss}^{-1}$  and a magnetic field of  $3.1 \times 10^{12} \text{ G}$ , an age of  $1.7 \times 10^4 \text{ yr}$  and a rotational energy loss of  $3.5 \times 10^{36} \text{ erg s}^{-1}$ .

The radio pulsar PSR B1951+32 was discovered in 1988 with a period of 39.5 ms in the radio synchrotron nebula CTB 80 [7]. From radio observations it is deduced that the object has a characteristic age of  $1.1 \times 10^5 \text{ yr}$ , a

surface magnetic field of  $4.9 \times 10^{11} \text{ G}$ , a rotation energy loss of  $3.7 \times 10^{36} \text{ erg s}^{-1}$  and it is located at  $1.5 \div 3 \text{ kpc}$  from Earth. It has been observed as an X-ray pulsar by *RXTE* and as a gamma ray pulsar by *EGRET* [8].

## II. OBSERVATION

The *Fermi*-LAT is a pair-production telescope. It consists of tungsten foil and silicon microstrip converter/trackers (pair conversion and track measurement); hodoscopic cesium iodide calorimeters (energy measurement); plastic scintillator anticoincidence detectors (charged-particle rejection); and a programmable trigger and data acquisition system. The LAT's excellent sensitivity stems from a large effective area ( $\sim 8000 \text{ cm}^2$ ), broad field of view (2.4 sr) and superior angular resolution. The LAT is sensitive to  $\gamma$ -rays in an energy from 20 MeV to 300 GeV.

Data used for this analysis were collected between August 2<sup>nd</sup>, 2008 and January 31<sup>st</sup>, 2009. In this period *Fermi* operated in sky survey mode scanning the sky every two orbits (approximately 3 hours). We selected only  $\gamma$ -ray events belonging to the *diffuse* class sample [1], that ensures the best background rejection, excluding those events coming from directions with a zenith angle in the Earth reference frame larger than  $105^\circ$  in order to avoid possible contamination from Earth albedo photons caused by cosmic rays interacting in the atmosphere.

## III. LIGHT CURVES

A temporal analysis of the photons arrival time for all the three pulsars has been performed using the timing solution provided by different radio telescopes [9].

All the three pulsars are embedded in the bright  $\gamma$ -ray emission of the Galactic plane, which is particularly strong and not well spatially resolved at low energies. Further, the LAT has an angular resolution dominated by scattering of low energies photons, like all pair production telescopes. The energy dependent cone of radius  $\theta_{68} \sim 0.8^\circ \text{ E}(\text{GeV})^{-0.75}$  is estimated to contain 68% of events. Thus selection of photons from an energy-dependent region of interest (ROI) around pulsar location is important; the best selection depends on the desired product. Here, we seek pulse profiles with good signal to noise over a broad energy range, so we select photons within an angle of  $\theta < \text{Max}(\theta_{68}, 0.35^\circ)$  of the pulsar position. This includes a larger fraction of high energies photons, where the background is relatively faint.

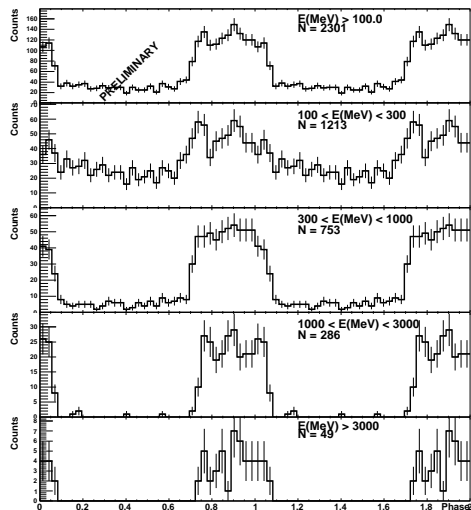


Fig. 1. Light curve for PSR B1055-52. Bin width of  $10^\circ$  rotation. No photons detected above 10GeV.

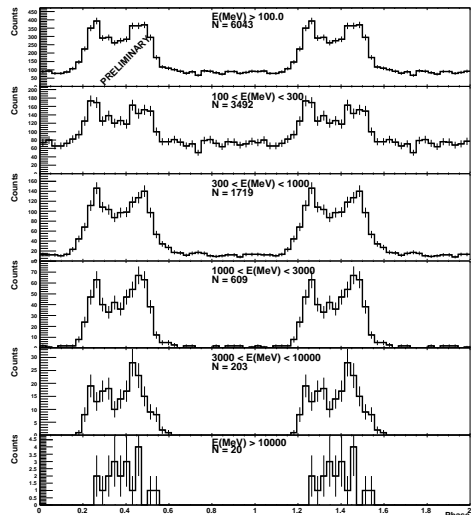


Fig. 2. Light curve for PSR B1706-44. Bin width of  $10^\circ$  rotation.

In Figures 1, 2 and 3 are shown the light curves for the three pulsars in different energy ranges. The timing solutions used are reported in Table I.

The light curve of PSR B1055-52 has been built using 2301 photons with  $E > 100$  MeV. It shows a complex emission pattern extending over about  $160^\circ$  of rotation; it is possible to observe two peaks, a narrow one from 0.7 to 0.8 in phase, and a wider one from 0.8 to 1.1 in phase. Probably the wider one hides the presence of two non completely resolved peaks (see especially the energy range  $1\text{GeV} < E < 3\text{GeV}$ ). The collected photons extend up to 10 GeV and there is no evidence of emission for  $E > 10\text{GeV}$ . The radio light curve at 1300Hz for this pulsar shows two peaks separated by half rotation: the 0 phase is defined by the highest peak. It is worthwhile to note that for this pulsar the first radio peak and the first gamma peak are aligned in phase.

On August 14<sup>th</sup>, 2008 a glitch occurred on PSR

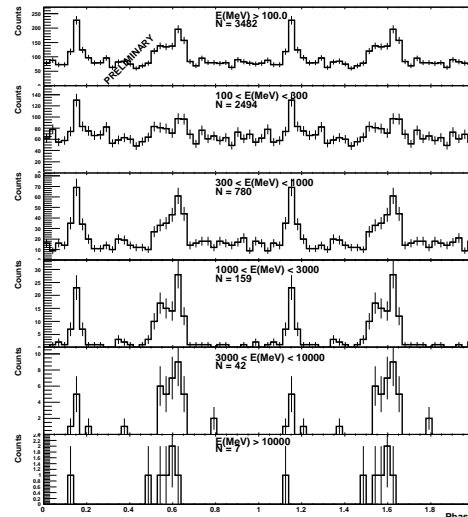


Fig. 3. Light curve for PSR B1951+32. Bin width of  $10^\circ$  rotation.

B1706-44, so the previous radio timing solutions are no more valid. The light curves have been built using a timing solution provided by Parkes valid from Sept 23<sup>rd</sup>, 2008 (40 days after the glitch) The light curve, built with 6430 photons with  $E > 100$  MeV, shows a two-peaks emission pattern over about  $145^\circ$  rotation in all the energy ranges up to  $E > 10\text{GeV}$ . The peaks range from 0.2 to 0.3 and from 0.4 to 0.55 in phase. The peak of the single radio pulse defines the 0 of the phase, and there is a shift of  $90^\circ$  between the radio peak and the first  $\gamma$  peak.

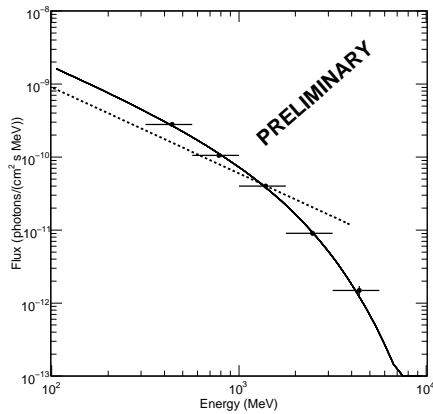
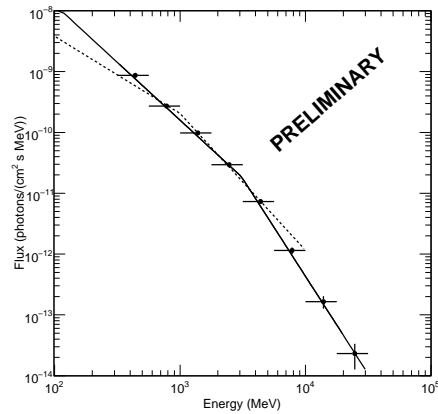
The light curve of PSR B1951+32 has been built using the timing solutions of the Nançay radio telescope with 3482 photons ( $E > 100$  MeV). The peak of the single radio pulse defines the 0 of the phase. There is a shift of  $55^\circ$  between radio peak and the first  $\gamma$  peak. It shows a light curve with two well separated peaks one from 0.1 to 0.2 and the other from 0.5 to 0.7 in phase (separation of  $160^\circ$  rotation). The second peak is wider than the first one and could hide the presence of another not separated third peak. The pulsation is clear up to  $E > 10\text{GeV}$ .

#### IV. GAMMA-RAY SPECTRA

The spectral analysis of the  $\gamma$ -ray emission was performed using a maximum-likelihood method ([10]) implemented in the *Fermi* SSC Science Tools. This method fits a source model to the data along with models for the instrumental, extragalactic and Galactic backgrounds. We selected photons in a  $15^\circ$  region around the pulsar radio position. The diffuse emission from the Galactic plane is modeled using maps based on the GALPROP code ([11], [12]), whereas the instrumental background and the extragalactic radiation are described by a single isotropic component with a power-law shape. Nearby sources in that field of view are extracted from the bright source list ([13]) and taken into account in the study. In this paper all the spectral analysis shown are phase averaged, but to enhance the pulsed signal

TABLE I  
 TIMING SOLUTIONS

Pulsar Name	B1055-52	B1706-44	B1951+32
Right Ascension (J2000)	10 <sup>h</sup> 57 <sup>m</sup> 58 <sup>s</sup>	17 <sup>h</sup> 09 <sup>m</sup> 42 <sup>s</sup>	19 <sup>h</sup> 52 <sup>m</sup> 58 <sup>s</sup>
Declination (J2000)	-52°26'56"	-44°29'08"	+32°52'40"
Pulse frequency (Hz)	5.0732281499	9.7563916566	25.2950092471
Frequency derivative (Hz s <sup>-1</sup> )	-1.50177×10 <sup>-13</sup>	-8.88280×10 <sup>-12</sup>	-3.73835×10 <sup>-12</sup>
Frequency 2 <sup>nd</sup> derivative (Hz s <sup>-2</sup> )	0	0	3.72019×10 <sup>-22</sup>
Epoch (MJD)	54561	54817	54400.25
Observatory	Parkes	Parkes	Nancay


 Fig. 4. Flux for pulsar B1055-52. • Fermi data, dashed line EGRET fit from [4], Solid line represents the fit of *Fermi* data.

 Fig. 5. Flux for pulsar B1706-44. • *Fermi* data, dashed line EGRET fit from [6], Solid line represents the fit of *Fermi* data.

with respect to the unpulsed one we have applied a low energy cut of 300MeV. Looking at the light curves of all the three pulsars it is clear that the unpulsed component is lower for  $E > 300\text{MeV}$ , so the obtained spectra are comparable with pulsed spectra.

To get the data points we have applied the maximum-likelihood method in all the individual energy bins in which we have divided our data. We have used 4 bins per decade in order to have enough photon statistics in each bin. We have chosen to discard from the plot all the points belonging to energy bins in which the source is not detected at level of at least of  $3\sigma$ . The error bars on the points reported in the figures take into account only statistical errors.

To check our results we have also applied an unfolding method ([14]), based on the Bayes's theorem, that allows to reconstruct the true energy spectrum from the observed one taking into account the dispersions introduced by the instrument response function. The data points obtained with this method are in good agreement with the ones from the maximum-likelihood method. The results from both these analysis are also consistent with those from the likelihood fit performed over all the data sample.

All the errors reported in this paper are statistical.

From the light curves in Figure 1 it is clear that pulsar B1055-52 emits up to  $E \sim 10\text{GeV}$ . In Figure 4 are reported the *Fermi* result compared with EGRET

ones. The EGRET data was fitted [4] with a simple power law with a spectral index of  $-1.18 \pm 0.16$ , while *Fermi* data seems to show a spectral behavior that could be fitted by a power law with exponential cutoff (Eq. 1). The result of the fit for  $E > 300\text{MeV}$  is  $N_0 = (1.36 \pm 0.14) \times 10^{-10}$  photons  $\text{cm}^{-2} \text{s}^{-1}$ ,  $\gamma = 1.18 \pm 0.11$  and  $E_c = 1.42 \pm 0.16\text{GeV}$ . The measured flux for  $E > 300\text{MeV}$  is  $1.69 \pm 0.05 \times 10^{-7}$  photons  $\text{cm}^{-2} \text{s}^{-1}$  and the energy flux is  $7.34 \pm 0.08 \times 10^{-10}$  ergs  $\text{cm}^{-2} \text{s}^{-1}$ . For comparison the EGRET flux was  $1.6 \pm 0.3 \times 10^{-7}$  photons  $\text{cm}^{-2} \text{s}^{-1}$

$$\frac{dN}{dE} = N_0 \left( \frac{E}{1 \text{ GeV}} \right)^{-\gamma} e^{-\frac{E}{E_c}} \quad (1)$$

Pulsar B1706-44 shows a different kind of spectrum with high energy emission detected up to 50GeV. For this pulsar both EGRET and *Fermi* data points are well described by a broken power law (Eq 2). *Fermi* fit result for  $E > 300\text{MeV}$  is  $N_0 = (1.86 \pm 0.38) \times 10^{-11}$  photons  $\text{cm}^{-2} \text{s}^{-1}$ ,  $E_b = 3.01 \pm 0.28 \text{ GeV}$ ,  $\gamma_1 = 1.91 \pm 0.03$  and  $\gamma_2 = 3.25 \pm 0.14$ , from which we can derive a flux for  $E > 300\text{MeV}$  equal to  $5.89 \pm 0.09 \times 10^{-7}$  photons  $\text{cm}^{-2} \text{s}^{-1}$  and an energy flux equal to  $8.25 \pm 0.19 \times 10^{-10}$  ergs  $\text{cm}^{-2} \text{s}^{-1}$ .

$$\frac{dN}{dE} = N_0 \begin{cases} \frac{E}{E_b}^{-\gamma_1} & E \leq E_b \\ \frac{E}{E_b}^{-\gamma_2} & E > E_b \end{cases} \quad (2)$$

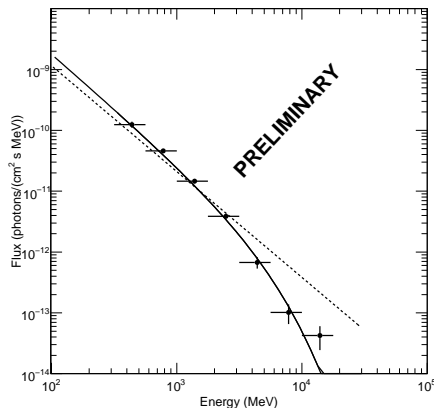


Fig. 6. Flux for pulsar B1951+32. • *Fermi* data, dashed line EGRET fit from [8], Solid line represents the fit of *Fermi* data.

EGRET parameters for the fit are  $N_0 = (2.05 \pm 0.19) \times 10^{-10}$  photons  $\text{cm}^{-2} \text{s}^{-1}$ ,  $E_b = 1 \text{ GeV}$  (fixed in the fitting procedure),  $\gamma_1 = 1.27 \pm 0.09$  and  $\gamma_2 = 2.25 \pm 0.13$ .

*Fermi* data show a higher energy break and harder spectral indexes than EGRET data, moreover *Fermi* extends the measured spectrum up to 30 GeV.

In Figure 6 is shown the spectrum for pulsar B1951+32. It emits up to 20 GeV and the spectrum is well fitted by a power law with an exponential cutoff (Eq. 1) The results of the fit are  $N_0 = (3.03 \pm 0.32) \times 10^{-11}$  photons  $\text{cm}^{-2} \text{s}^{-1}$ ,  $\gamma = 1.78 \pm 0.14$  and  $E_c = 4.31 \pm 1.27 \text{ GeV}$ . Only the last point seems to be completely out from the fit line. The flux for  $E > 300 \text{ MeV}$  is  $7.23 \pm 0.44 \times 10^{-8}$  photons  $\text{cm}^{-2} \text{s}^{-1}$  and the energy flux is  $1.10 \pm 0.06 \times 10^{10}$  ergs  $\text{cm}^{-2} \text{s}^{-1}$ .

EGRET data instead were fitted with a simple power law with spectral index equal to  $-1.74 \pm 0.11$ . Also in this case the spectrum obtained from *Fermi* data is more complex than the simple power law from EGRET analysis.

## V. CONCLUSION

In 6 months of sky survey operation *Fermi*-LAT has increased the photon statistic for the three EGRET pulsars described in this proceeding of almost an order of magnitude. These results added with the excellent timing capability of *Fermi* allowed to obtain light curves that show complex emission patterns that can give useful hints for the modeling of the pulsars.

The new spectra obtained are different and more accurate than the ones obtained by fitting EGRET data. For the pulsars B1055-52 and B1952+32 the spectrum is well described by a power law with exponential cut off rather than a simple power law, for B1706-44 the spectrum is always fitted by a broken power law but with an higher energy break and harder spectral indexes.

Emission models fall into two classes: Polar cap (PC) scenarios [15], which place the emission very close to

the star surface, and outer magnetosphere models (outer gap (OG) [16] and Slot Gap (SG) [17]) which predict the high energy pulsed emission originates at high altitudes extending towards the light cylinder.

Gamma-rays created at the polar caps interact with the intense magnetic fields near the neutron star surface, resulting in superexponential spectral cut-offs below a few GeV, while OG models predict simple exponential cutoffs.

LAT data for B1706-44 confirm and refine the spectral break measured with EGRET while for B1952+32 the observed emission beyond 10 GeV and absence of a sharp cut-off indicate outer magnetosphere processes. In the case of B1055-52 the emission is lower than 10 GeV but no sharp cut off is measured and also for this pulsar a magnetosphere processes is favored.

Another observation in support of the high latitude  $\gamma$ -rays emission is the appreciable offset from the single radio peak (at least for B1704-44 and B1951+32) and the gamma peaks in the light curves, as expected in the case of high magnetosphere processes.

## VI. ACKNOWLEDGMENT

The *Fermi* LAT Collaboration acknowledges support from a number of agencies and institutes for both development and the operation of the LAT as well as scientific data analysis. These include NASA and DOE in the United States, CEA/Irfu and IN2P3/CNRS in France, ASI and INFN in Italy, MEXT, KEK, and JAXA in Japan, and the K. A. Wallenberg Foundation, the Swedish Research Council and the National Space Board in Sweden. Additional support from INAF in Italy for science analysis during the operations phase is also gratefully acknowledged. The Parkes radio telescope is part of the Australia Telescope which is funded by the Commonwealth Government of operation as a National Facility managed by CSIRO. The Nançay Radio Observatory is operated by the Paris Observatory, associated with the French Centre National de la Recherche Scientifique (CNRS). We thank our colleagues for their assistance with the radio timing observations.

## REFERENCES

- [1] Atwood, W. B., et al., 2009, accepted by ApJS, arXiv:0902.1089
- [2] Vaughan, A.E. & Large, M.I., 1972, MNRAS, 156, 27P
- [3] Cheng, A.f. & Helfand, D.J., 1983, ApJ, 271, 271
- [4] Fierro, J.M. et al., 1993, ApJ 413, 27
- [5] Johnston, S., Lyne, A.g., Manchester, R.N., Kniffen, D.A., D'Amico, N., Lim, J. & Ashworth, M., 1992, MNRAS, 255, 401
- [6] Thompson, D.J. et al., 1996, ApJ 465, 385
- [7] Kulkarni, S.R., et al., 1995, Nature, 331, 50
- [8] Ramanamurthy, P.V. et al., 1995, ApJ 447, 109
- [9] Smith, D.A. et al. A&A, 2008, 492, 923
- [10] Mattox, J.R. et al., 1996, ApJ, 461, 396
- [11] Strong, A.W., Moskalenko, I.V. & Reimer, O., 2004, ApJ, 613, 962
- [12] Strong, A.W., Moskalenko, I.V., Reimer, O. Digel, S., & Diehl, R., 2004, A&A, 422, L47
- [13] Abdo, A.A. et al., 2009, ApJ, submitted (arXiv/0902.1340)
- [14] Mazziotta, M.N. A method to unfold the energy spectra of point like sources from the *Fermi*-LAT data This proceedings
- [15] Daugherty, J. K. & Harding, A. K. 1996, ApJ, 458, 278
- [16] Romani, R. W. & Yadigaroglu, I.A. 1995, ApJ, 438, 314
- [17] Arons, J. 1983, ApJ, 266, 215